

Appendix S1: Estimation of acoustic exposure in seals

Source characteristics

The median broadband peak-to-peak source level (235 (SD=14.6) dB re 1 μ Pa @ 1m) reported during previous pile driving at the same wind farm prior to this seal study (Nedwell, Brooker & Barham 2011) was used as a broadband source level for pile driving; this was assumed to be for the maximum blow energy of the downward stroke of piling hammer used during the installation (2,000 kJ). Previous studies have shown that source level of pile driving varies with blow energy. For example, Bailey *et al.* (2010) reported a linear relationship between blow energy and peak-peak source level during the installation of 1.8 m diameter piles. We therefore corrected the source level for changes in blow energy by relating information on the timing and blow energy of individual piling strokes (provided by wind farm developer) with information on the received levels of individual pulses recorded using an autonomous moored sound recorder (DSG-Ocean Acoustic Datalogger; Loggerhead Instruments, FL, USA). This recorder was moored at a range of 4,900 metres from the pile driving location.

Peak-to-peak sound pressure levels ($SPL_{(p-p)}$) were measured for all pile driving pulses recorded on the sound recorder (2,213 pulses); all acoustic analyses were carried out using Adobe Audition (Version 2.0; Adobe Systems Inc.) and MATLAB (Version R2011b 7.13.0.564; Mathworks Inc). The received $SPL_{(p-p)}$ for each pulse was then temporally matched to the associated blow energy (Figure S2) and the relationship between them was analysed using a generalised linear model with a Gaussian error distribution in the statistical package R (R Development Core Team (2012). R: A language and environment for statistical computing. R Foundation for Statistical Computing, Vienna, Austria. ISBN 3-900051-07-0, URL <http://www.R-project.org>); the best fit model was described by $3.8 \times \ln(\text{blow energy})$ relationship ($\chi^2_{1,2211}=10,447, P<0.0001$). The predicted source levels were therefore described using Equation S1.

(Equation S1)

$$SL_{(energy\ corrected)} = SL + 3.8 \times \ln\left(\frac{\beta}{\beta_{max}}\right)$$

Where: SL is 235 dB re 1 μ Pa at 1m [median predicted peak-to-peak source level from (Nedwell, Brooker & Barham 2011)];

β_{max} is the maximum blow energy (2,025) of the pile driving in kilojoules (kJ);

β is the blow energy of the pile driving stroke in kilojoules (kJ);

Acoustic impact is not only affected by peak pressure, but also by the energy flux density (or sound exposure level: SEL) of the sound pulse (Ward 1997). Therefore, the SEL of the source level [given by integrating the duration of the signal and the pressure squared (Urick 1983)] was estimated using Equation S2. The difference between the peak-to-peak and the root mean square (RMS) levels was calculated as a mean value from twenty pile driving pulses recorded on the autonomous recorder; this was 16.2 dB (SD=1.6). Similarly, the mean duration of the pulses [defined as the region of the waveform containing the central 90% of the energy of the pulse (Lucke *et al.* 2009)] (e.g. Figure S1) was calculated from the same twenty recorded pile driving pulses; this was 0.157 (SD=0.02) seconds. Using these approaches, the pile driving was estimated to have a maximum single-pulse SEL of 211 dB re 1 μ Pa²-s (at a blow energy of 2,000kJ).

(Equation S2)

$$E = 10 \log \int_{t_5}^{t_{95}} p^2(t) dt$$

Where E is the energy flux density (dB re: $1 \mu\text{Pa}^2 \text{ s}$);
 $p(t)$ is the instantaneous pressure in Pascals (Urick 1983);
 t is time in seconds;
 t_5 and t_{95} are the times between which 90% of the energy is contained;

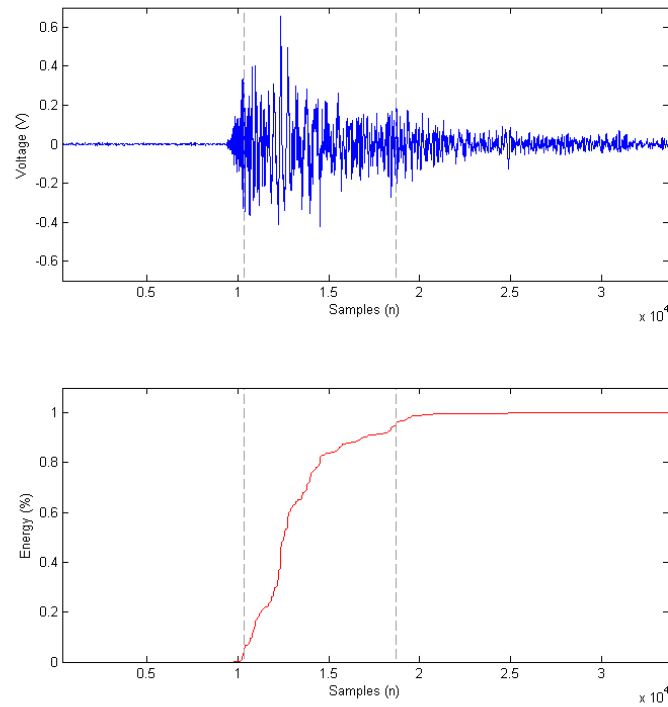


Figure S1: Figure showing the waveform of a single pile driving pulse recorded on an autonomous sound recorder (DSG-Ocean Acoustic Datalogger; Loggerhead Instruments, FL, USA) (upper) moored approximately 5km from the pile driving. The duration of the pulse was defined as the region of the waveform containing the central 90% of the energy of the pulse (lower); in this case, the duration was 16,700 samples (0.17 seconds). This approach was used to calculate the mean pulse duration of twenty pile driving pulses.

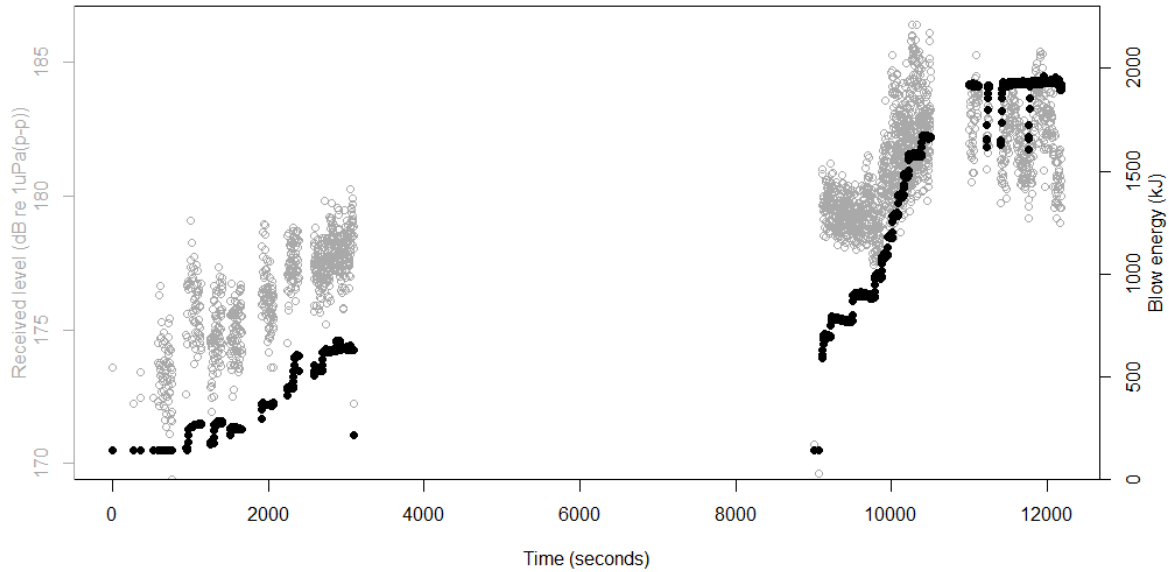


Figure S2: Blow energy (kJ) of each pile driving stroke (grey points) and received sound pressure levels (dB re $1\mu\text{Pa}_{(p-p)}$) of each pile driving pulse recorded on an autonomous sound recorder (DSG-Ocean Acoustic Datalogger; Loggerhead Instruments, FL, USA) (black points) moored 4,900 m from the pile driving.

Transmission loss

Transmission loss across the study area was then estimated using a series of range dependent acoustic models (Collins 1993) which accounted for the geoacoustic properties of the water column and seabed (Jensen *et al.* 1994); modelling was carried out using the RAMSGeo model in the MATLAB Acoustic Toolbox User interface and Post processor (ActUP V2.2L; Curtin University, Australia). This is based on a split-step Padé solution to the parabolic equation (Collins 1993) and is appropriate for modelling low frequency transmission loss in range dependent environments (Collins 1993; Duncan & Maggi 2006); its implementation in the MATLAB toolbox is described in detail by Duncan and Maggi (2006). The study area is a large open bay that extends northeast into the North Sea. Water depths are relatively shallow throughout with several large submerged sandbanks present. Information on water depth was taken from Edina Marine Digimap® (Crown Copyright/SeaZone Solutions. All Rights Reserved. 052006.001 31st July 2011). Seabed sediment types across the study area are relatively homogenous being primarily sand (59.3% of the area) with a lower proportion of areas classed as gravelly-sand (19.5%) and sandy-gravel (13.4%); the remaining 7.8% consists primarily of muddy-sand and gravel (sediment data used with permission of the British Geological Survey <http://www.bgs.ac.uk/>). Other parameters used to specify the propagation models are shown in Table S1.

Table S1: Parameters used in the RAMSGeo transmission loss models.

RAMSGeo parameter	Value
Relative range resolution (*dz)	2
Reference phase velocity (ms ⁻¹)	1,467
Number of terms in the Padé expansion	6
Irot	0
Theta	0
Attenuation layer thickness (lambda)	10
Attenuation layer maximum s-wave attenuation (dB/lambda)	10
Minimum sheer velocity in substrate (ms ⁻¹)	10

Transmission loss was calculated at the peak frequency of the pile driving [200Hz: (Nehls *et al.* 2007)] at 1km intervals along 5 degree radii from each of the pile driving source locations out to a range of 200 km (Figure S). At each 1km interval, transmission loss at a series of water depths was estimated; these were one metre and each five metre depth interval from five to 110 m depth (i.e. maximum seal dive depth during the study) (Figure). Water depths at each of the pile driving locations ranged from 8.0 to 20.8 m (mean =12.2m, SD= 3.1m). The depth of the source was defined as the middle of the water column at each piling location. Further, given the majority of pile driving in the current study occurred primarily during winter and early spring, for modelling purposes, the water column was assumed to be non-stratified with respect to salinity and temperature (Richardson & Bo Pederson 1998).

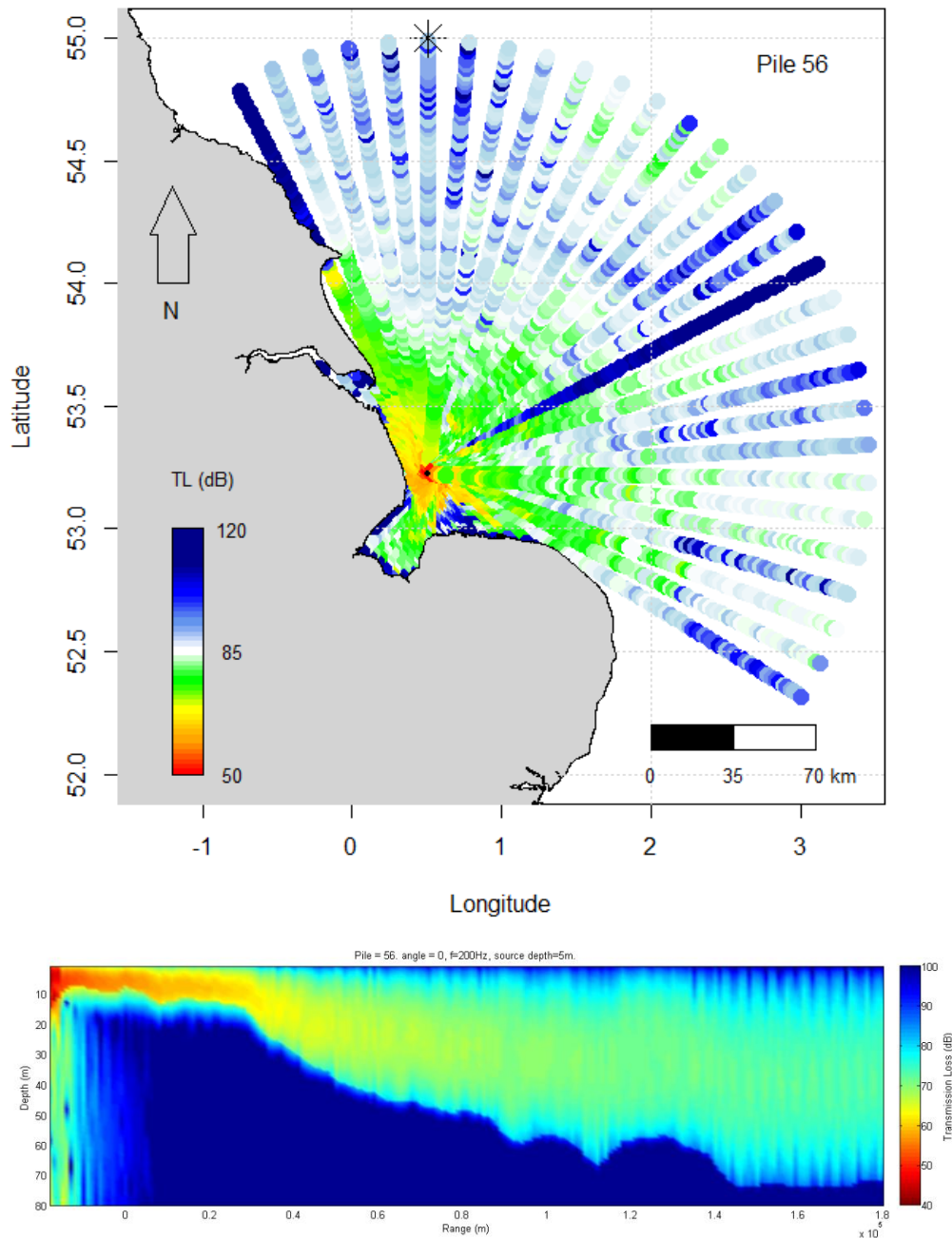


Figure S3: Example of the spatial pattern in predicted transmission loss (dB) of pile driving sound around the study area for one of the piled foundations (#56: 53.12877°N, 0.47923°W; water depth at source = 5 m). The upper panel shows the location of one of the piled foundations (black point) and the associated transmission loss estimates at a depth of 1 m and at 1 km intervals along 72 transects out to 200 km. The lower panel shows an example of the associated depth related transmission loss along one of the transects (denoted by the asterisk at the end of the transect) shown in the upper figure. It should be highlighted that the colour scales on each panel have different ranges associated with them.

The estimated energy corrected source levels and transmission loss models were validated using a series of boat based calibrated recordings during the installation of one of the piles; these recordings effectively covered the full range of pile driving blow energies (142-1,960 kJ). Recordings were made using a Reson TC 4014 hydrophone deployed at approximately 1 m

depth with a Brüel and Kjaer Amplifier (type 2635) and a calibrated Avisoft ultrasoundgate 416 digital acquisition system at a sample rate of 192 kHz. Recording locations varied between 1,000 and 9,500 m from the pile driving (Figure S3). Post-hoc analyses of 710 piling strokes were carried out to validate the predicted individual pulse SELs. Examples of the waveforms and spectrograms of the pile driving are shown in Figure S3S.

Measured single pulse SELs from the boat based recordings varied from 130.0 to 142.8 dB re 1 $\mu\text{Pa}^2\text{-s}$ with a mean of 135.4 (SD=3.2) dB re 1 $\mu\text{Pa}^2\text{-s}$; predicted values varied from 135.3 to 142.1 dB re 1 $\mu\text{Pa}^2\text{-s}$ with a mean of 137.7 (SD=1.8) dB re 1 $\mu\text{Pa}^2\text{-s}$. Comparison of the measured SELs with their corresponding predicted SELs showed that the errors (where a positive value represents an overestimate and a negative value an underestimate) ranged from -4.3 to +9.6 dB re 1 $\mu\text{Pa}^2\text{-s}$ (Figure S4). Overall mean error was +2.3 dB re 1 $\mu\text{Pa}^2\text{-s}$ and overall mean root-squared error was 2.9 dB re 1 $\mu\text{Pa}^2\text{-s}$. Median error at each range varied from -1.2 at a range of 3km to 6.5 dB re 1 $\mu\text{Pa}^2\text{-s}$ at a range of 7.7km; median error was positive at the majority of recording ranges (Figure S5).

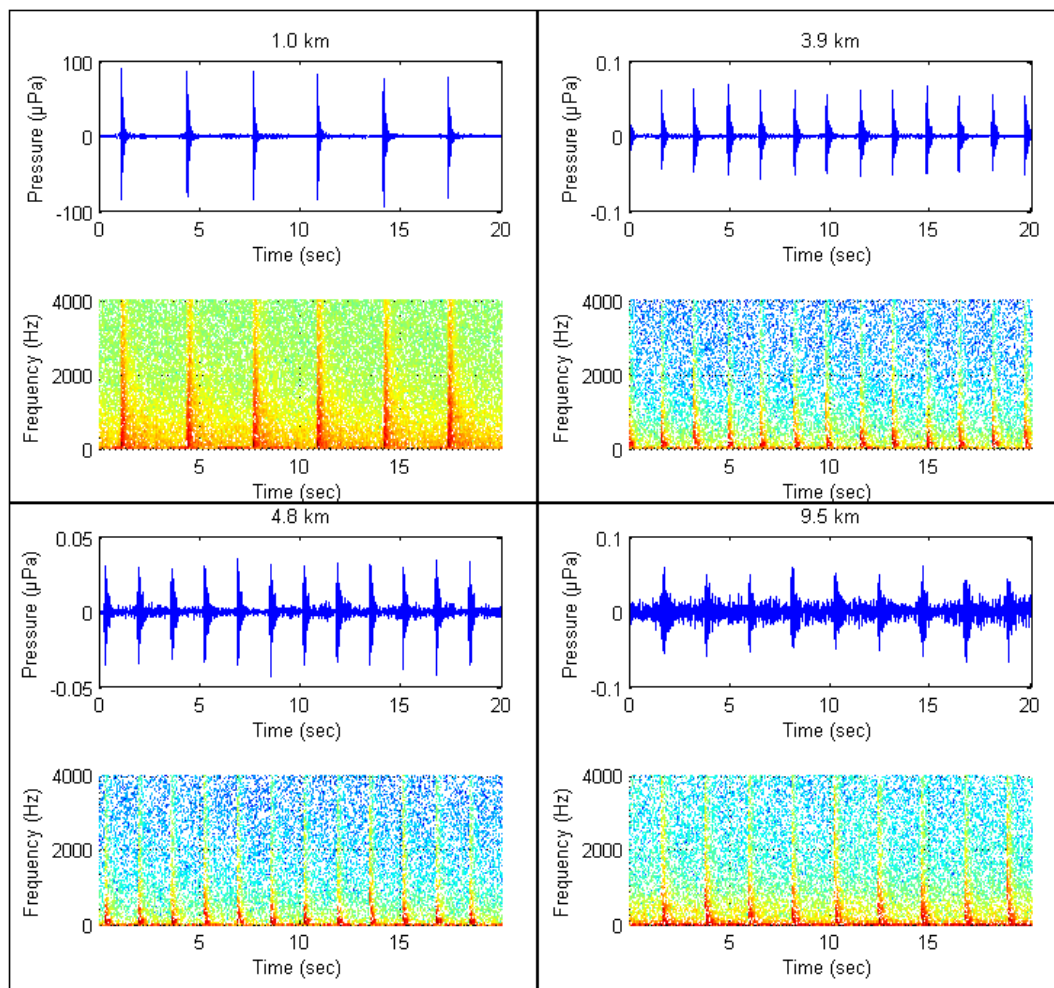


Figure S3: Examples of the waveforms and spectrograms (FFT size: 4096, time resolution: 10.7 ms, number of FFT steps: 2048, weighting function: Hamming window) of pile driving recorded at a series of ranges from the piling location. The figure shows a total of 20 seconds of pile driving recorded at 1.0 (top left), 3.9 (top right), 4.8 (bottom left), and 9.5 (bottom right) km from the piling location.

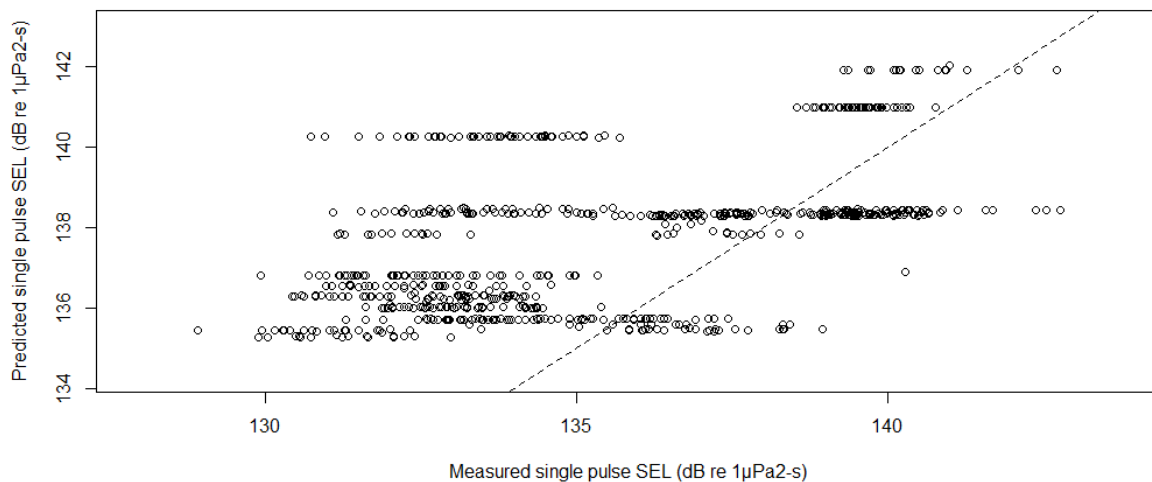


Figure S4: The acoustic modelling approaches were validated using a series of boat based calibrated recordings during the installation of one of the piles; this plot shows the measured single pulse Sound Exposure Levels (SEL: dB re 1 $\mu\text{Pa}^2\text{-s}$) for a total of 710 pile driving pulses on the x axis and the predicted SELs based on the source terms and transmission loss models on the y axis. For reference, the dashed line represents the line of equality.

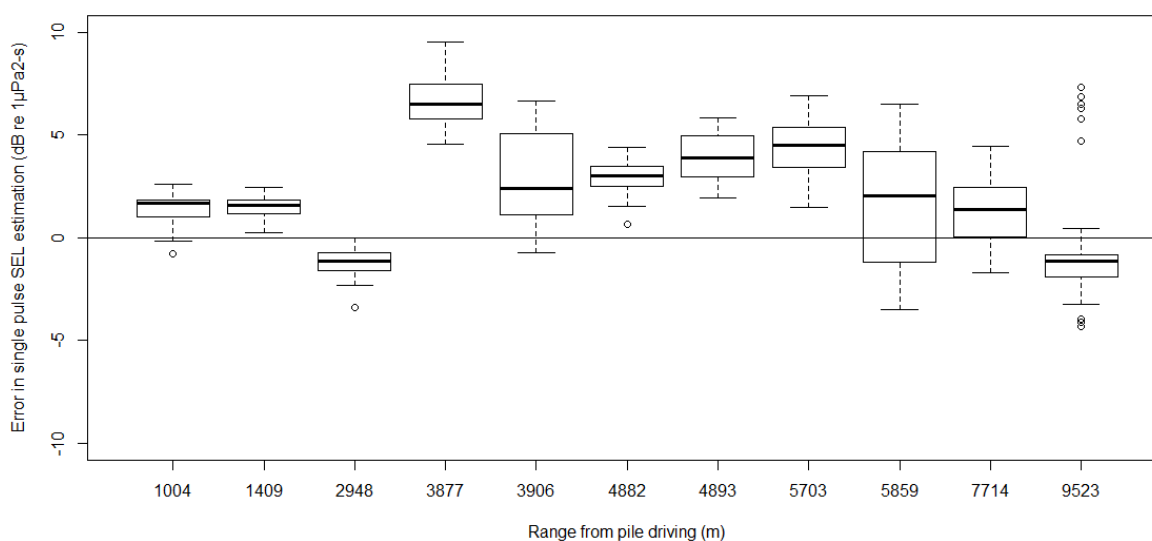


Figure S5: Boxplot of the error in single pulse Sound Exposure Level (SEL: dB re 1 $\mu\text{Pa}^2\text{-s}$) estimation with range from the pile driving location (where a positive value represents an overestimate and a negative value an underestimate). Median error at each range varied from -1.2 at a range of 3km to 6.5 dB re 1 $\mu\text{Pa}^2\text{-s}$ at a range of 7.7km; median error was positive at the majority of recording ranges.

References

- Bailey, H., Senior, B., Simmons, D., Rusin, J., Picken, G. & Thompson, P.M. (2010) Assessing underwater noise levels during pile-driving at an offshore windfarm and its potential effects on marine mammals. *Marine Pollution Bulletin*, **60**, 888-897.
- Collins, M.D. (1993) A split-step Pade solution for the parabolic equation method. *Journal of the Acoustical Society of America*, **93**, 1736-1742.
- Duncan, A.J. & Maggi, A.L. (2006) A consistent, user friendly interface for running a variety of underwater acoustic propagation codes. *Proceedings of ACOUSTICS 2006. 20-22 November, 2006, Christchurch, New Zealand. Available from: http://www.acoustics.asn.au/conference_proceedings/AASNZ2006/papers/p29.pdf.*
- Jensen, F., Kuperman, W., Porter, B. & Schmidt, H. (1994) *Computational Ocean Acoustics*. Springer-Verlag, New York.
- Lucke, K., Siebert, U., Lepper, P.A. & Blanchet, M.-A. (2009) Temporary shift in masked hearing thresholds in a harbor porpoise (*Phocoena phocoena*) after exposure to seismic airgun stimuli. *Journal of the Acoustical Society of America*, **125**, 4060-4070.
- Nedwell, J.R., Brooker, A.G. & Barham, R.J. (2011) Measurement and Assessment of Underwater Noise during Impact Piling Operations at the Lincs Offshore Wind Farm. pp. 49. Subacoustech Environmental Ltd, Hants, UK.
- Nehls, G., Betke, K., Eckelmann, S. & Ros, M. (2007) Assessment and costs of potential engineering solutions for the mitigation of the impacts of underwater noise arising from the construction of offshore windfarms. *BioConsult SH report, Husum, Germany. On behalf of COWRIE Ltd.*
- Richardson, K. & Bo Pederson, F. (1998) Estimation of new production in the North Sea: consequences for temporal and spatial variability of phytoplankton. *Ices (International Council for the Exploration of the Sea) Journal of Marine Science*, **55**, 574-580.
- Urick, R.J. (1983) Principles of underwater sound. *3rd ed.*, New York. 423 pages.
- Ward, W.D. (1997) Effects of high intensity sound. *Encyclopedia of Acoustics*, pp. 1496-1507. Wiley, New York.